Sigma Journal of Engineering and Natural Sciences
Web page info: https://sigma.yildiz.edu.tr
DOI: 10.14744/sigma.2026.2032

Research Article

# Optimized mix framework for accelerated carbonation concrete by ground granulated blast furnace slag and silica fume

**Ramatai B. SOMWANSHI[1,*], Abhijeet R. NARDEY[1], Padmanabh Arun GADGE[2]**

[1]*Department of Civil Engineering, G H Raisoni University, Madhya Pradesh, 480337, India*
[2]*Department of Mechanical Engineering, G H Raisoni University, Madhya Pradesh, 480337, India*

## ARTICLE INFO

*Article history*
Received: 27 December 2024
Revised: 20 March 2025
Accepted: 21 March 2025

**Keywords:**
Acid Attack; Carbonation Concrete; Chloride Permeability; Compression Strength; Taguchi Optimization

## ABSTRACT

The proportion of carbon dioxide in the atmosphere has risen enormously, particularly in the last decade. The carbon sequestration technique reduces the carbon dioxide level in the atmosphere. One such method in concrete technology is carbonation curing of concrete during its early strength developing age. During accelerated carbonation, the un-hydrated particles in the concrete combine with carbon dioxide and form carbonate, leading to the accelerated solidification of concrete with improved durability properties. However, if the mix is not selected properly, then it takes a longer curing time than other traditional mixes. Hence, selecting the optimal mix based on the desired outcome and less curing time has tended to gain the finest mechanical properties. In this investigation, a novel approach, termite-based Taguchi optimization, is implemented to predict the mix proportion of concrete from the material parameters of the concrete. Before, the termite model was not implemented for this specific application, nor was Taguchi optimization. The fitness function in the Termite algorithm helps with carbonation curing of the concrete, and the prediction function is executed to determine the endurance parameters of the concrete, which is considered a novelty of the study. The endurance of the carbonation concrete is determined in terms of compression strength, carbonation depth, chloride permeability, water sorptivity, and acid attack. Moreover, the important results are the mix containing 15% silica fume and 60% Ground Granulated Blast Furnace Slag has lower results in the permeability tests of concrete that include Carbonation depth of 4mm, water sorptivity of 0.0125 mm/sec$^{0.5}$ and 619.25 coulombs in the chloride permeability test at the 28$^{th}$ day. In strength parameters, the mix containing 15% silica fume and 40% Ground Granulated Blast Furnace Slag possesses higher compression strength of 47 MPa and strength reduction in the acid attack test of 6.26% at the 28-day test. Since, the mix proportion with 15% silica fume and 40% Ground Granulated Blast Furnace Slag possess higher strength and optimal permeability values. This mix is considered an optimum mix for this research.

**Cite this article as:** Somwanshi RB, Nardey AR, Gadge PA. Optimized mix framework for accelerated carbonation concrete by ground granulated blast furnace slag and silica fume. Sigma J Eng Nat Sci 2026;44(2):1153−1171.

***Corresponding author.**
*E-mail address: ramataibabaraosomwanshirbs@gmail.com

*This paper was recommended for publication in revised form by Editor-in-Chief Ahmet Selim Dalkilic*

Published by Yıldız Technical University Press, İstanbul, Turkey

## INTRODUCTION

The industrialization and urbanization that have taken place in recent decades have been greatly influenced by the building industry [1]. The construction sector generates 5–10% of all jobs worldwide and contributes 5–15% of GDP to each country [2]. The building industry accounts for about 30% of total resource depletion and 40% of overall energy use [3]. Moreover, these construction sectors generate over 30% of the world's waste and 40% of its carbon dioxide emissions [4]. The production of this cement was considered the main reason for carbon dioxide emissions across the globe, and the percentage of emissions was between 7 and 9 [5]. Currently, more than 5% of carbon dioxide emissions globally come from manufacturing facilities of cement production [6]. By using different binding elements in place of OPC, cementation materials can help lower carbon dioxide emissions [7]. Multiple industry wastes can be used in multi-component binder materials for various applications [8]. Much research has been done on concrete construction employing additives to lower the cost and scarcity of common materials [9]. In the building industry, cement is an essential part of concrete, the manufactured resource used in construction most frequently [10]. Approximately 4 billion tonnes of cement are produced annually worldwide, which translates to nearly 29 billion tonnes of concrete in 2015 [11]. The demand for cement is expected to expand steadily between 1990 and 2030. Considerable expansion in production has resulted from the rising demand for cement in modern infrastructure and structures, especially in emerging nations like China, Russia, and Japan [12]. Cement production has developed a capacity for generating 59.5 million tonnes of annual cement due to the anticipation of future demand for expanding infrastructure [13]. Cement prices have increased by almost 150% in the last ten years. As a result, it is crucial to use additional materials whenever possible in place of cement [14]. In the last thirty years, the building industry, especially in the United Kingdom, has taken some actions to minimize the release of toxic gases associated with cement production [15].

Alternatively, consider calcining coal using organic gas instead of petrol, absorbing carbon dioxide with chemicals, creating a more effective clinker grinding method, and implementing sustainable cement production [16]. However, cementitious materials might be a workable plan to cut greenhouse gas emissions dramatically [17]. Waste materials from manufacturing processes, like fly ash a byproduct from power plants, metakaolin, ground granulated blast furnace slag (GGBS), and fumes of silica, are utilized in place of OPC and can significantly reduce greenhouse gas emissions [18]. The particles of pozzolanic can be created through the buildup of chemical materials, such as silica, calcium, alumina, magnesia, and iron, into concentrations of more than seventy percent, according to ASTM [19]. GGBS contains over 70% of several elements, including iron, silica, calcium, alumina, and magnesia [20]. Therefore, fly ash, metakaolin, and GGBS silica fume can utilize the pozzolanic material, which might be used in concrete to replace OPC. Because of their binding qualities, these wastes silica fume, metakaolin GGBS, and fly ash, have drawn attention from researchers as potential additions to cement blends that could reduce the carbon dioxide quantity left on the bottom layers of the atmosphere [21]. Binding material can be used with other byproducts from industries, including rubber, fly ash, slag, foundry sand, waste marble, etc. The majority of these pozzolanic materials originate from manufacturing waste [22].

Industrial wastes, such as slag from the blast furnace and its sub-product GGBS, are most widely used as auxiliary materials in cement-based products for the production of concrete and cement [23]. Apart from its pozzolanic effect, its self-hydration characteristic sets it apart from other compounds [24]. Its color alters to the presence of 30–40% with the oxides of calcium. The certainty that GGBS will be an eco-friendly alternative for the binder in the concrete accounts for its significance [25]. GGBS needs to be disposed of properly because it is a byproduct. By mixing it with fine and coarse aggregates, OPC, and other conventional concrete components, this waste material can reduce its depletion from the concrete mix [26].

Cement-based materials can perform much better and store $CO_2$ permanently if their carbonation is accelerated. Research indicates that cement-based products cured by $CO_2$ have greater mechanical performance and durability, while recycled concrete aggregates treated by $CO_2$ have better qualities than untreated RCAs. Cement has considerable potential to store $CO_2$, as it can absorb up to 50% of its mass. Cement-based products have reduced $CO_2$ emissions by over 40%, sequestering 1.4 Gt of $CO_2$. Volume stability of carbonation-exposed cement-based composites is a concern due to cracking risk. Dimensional stability is less studied than mechanical properties, carbonation depth, and $CO_2$ uptake capacity. Advancements in microscope and spectroscopic technologies have led to the increased investigation into the carbonation process of cement hydration products and their microstructural impacts on concrete matric. Understanding these variations is essential for intelligent $CO_2$ sequestration and utilization technologies. Some alternative methods of lessening $CO_2$ emissions and streamlining concrete-making processes are capturing and utilizing flue gases produced in making cement, stimulating energy-efficient technology in cement manufacture, recycling and utilizing industrial residues, and investigating cement-free building practices. In particular, inorganic $CO_2$ sequestration has emerged as a relatively innovative mechanism for $CO_2$ reduction, promoting significant progress and environmental outcomes over the past two decades. Mineral $CO_2$ sequestration in concrete production can defined as a carbon capture and storage method that essentially entails $CO_2$ reacting with calcium-containing material to produce calcium carbonates. When atmospheric carbon dioxide reacts with the alkaline components of concrete, mainly portlandite, and the hydrated calcium silicate (CsSsH) gel, calcium carbonate ($CaCO_3$) is produced. This process is known as carbonation in concrete. The pH level in the pore water of the concrete usually drops due to this chemical reaction, going from extremely alkaline levels over 12 down below 8. The passive layer may be compromised if this reaction spreads to the steel reinforcement, leaving the steel vulnerable to possible corrosion.

Moreover, multiple studies have demonstrated that GGBS replacement in the binder of concrete will not decrease the strength of concrete [27]. Some of the research gaps found in the past literature are:

The carbon emission from the cement sector in India is considered a major source of a sustainable substitute to Portland cement. Materials activated by alkali solutions, including fly ash and GGBS are being investigated by Pandit et al. [28]. These materials have a good chemical composition, are easily accessible, and can be used to repurpose waste effectively. However, occasionally, it might impact the carbonation's passive layer and reduce its passivity.

The carbonation performance of Geopolymer Concrete (GPC), a sustainable green material for civil engineering that is comparable to Portland Cement (OPC), is introduced by Zhao et al. [29]. The merits, mechanism of the carbonation technique, and the evaluation techniques of GPC are presented, along with the correlation of the carbonation characteristics of the GPC with OPC, as well as an analysis of the factors influencing GPC's performance. Additional numerical models are recommended to increase the robustness and lifespan of GPC carbonation. On the other hand, it has an impact on the carbon dioxide content and the cement-to-water ratio

Sun et al. [30] examine replacing regular Portland cement (OPC) with a Slag of carbide (SC) as a catalyst in the excess-sulfate-based phospho-calcium sulfate dihydrate slag cement (EPSC). According to the results, increased SC doping causes low latest strength and an unstable hydration rate, while lower SC dosage lengthens the induction period and improves the final strength. In EPSC applications, a pH range of 11.00–11.75 provides the best hydration conditions for SC, guaranteeing both stability and effectiveness of hydration. On the other hand, air pressure and relative humidity following carbonation may result in certain uncommon situations.

The energy usage and emission of carbon dioxide in cement production led to environmental pollution. Two supplemental materials with cement characteristics (SMC) are added to the concrete to lower energy consumption fly ash (FA) and silica fume (SF). Using FA and SF as SMCs, Padavala et al. [31] focus on creating sustainable concrete in this work. Cement was used to replace FA and SF in two different mixes that were created. Other areas of study included sustainability index, mechanical characteristics, microstructure analysis, and cost-benefit analysis. Nevertheless, there are cases where the concrete cover reinforcement raises the possibility of corrosion.

Thorne et al. [32] investigate how low-carbon concrete with additional cementitious materials (SCMs) affects the environment. According to the results, adding fly ash admixture and limestone lowered carbon emissions but did not affect mechanical qualities. The study offers guidance for creating concrete materials that take into account the availability of nearly carbon-free concrete ingredients on a worldwide scale. Though concrete naturally has a high compressive strength, it is more expensive.

The research gaps that need to be addressed are poor compressive strength, poor bulk density, and other poor mechanical properties exposed in Table 1. This present study needed to use different types of municipal solid wastes and agricultural ashes to replace regular Portland cement, either entirely or partially, which has been relatively minimal and primarily limited to GGBS and pulverized fly ash PFA. Due to the negative environmental effects

**Table 1.** Summary of literature review

| Authors | Methods | findings | Research gaps |
|---|---|---|---|
| Pandit et al. [28] | GGBS with alkali treatment | The compressive strength of GPC is decreased by 5%, and the slag blend was expanded by 0.0963% | Passivity was decreased due to the impact of carbonation. |
| Zhao et al. [29] | GPC-anti carbonization | Carbonization PH11.23for 28 days with sodium concentration 3% | The carbon emission was too high |
| Sun et al. [30] | sulfate phosphogypsum slag cement | The hydration environment measured 11 to 11.75PH value, the attained suitable hydration environment 1.3% carbide slag | Durability strength is too low. |
| Padavala et al. [31] | supplementary cementitious materials with SF | The compressive strength 50Mpa recorded for 7.5% SF and 30% fly ash | Flexural strength is too low |
| Thorne et al. [32] | supplementary cementitious materials | Higher durability strength by 20.5% and reduced $C0_2$ 21.1%. | Chloride permeability was high. |

of burning coal and producing steel, it will soon be more difficult to find GGBS and PFA. GGBS causes concrete to become more carbonated, but at a faster rate as its content increases. This phenomenon is comparable to the fly ash effect. Compared to Portland cement (PC) concrete, this effect is stronger for concrete designed on an equal water/cement (w/c) ratio. The fast phase-out of fossil fuels in coal-fired power plants and steel manufacture and the serious environmental effects accompanying it are making it harder to find GGBS and FA these days. This study's importance is to replace OPC entirely or partially (using alkali activation technology) with other SCMs, such as ashes from volcanoes, woods, or agricultural ashes, as well as municipal solid wastes like glass trash and burned ashes.

The originality and novelty of this study is implementing the hybrid optimization model based on termite and taguchi for finding the optimal mix ratios that give desired mechanical properties in less curing time. The steps to proceed with the novelty solution are described below,

- Initially, the material parameters are defined in the orthogonal array of the system.
- The material parameters are assigned to the novel Termite-based Taguchi Optimization (TbTO) based on the major, minor, and intermediate conditions.
- The novel approach is intended to use finite optimization characteristics and prediction features to enhance quality without altering the quantity.
- Finally, the prediction function generates the key metrics in the optimized concrete, which are analyzed as compression strength, carbonation depth, permeability, and acid attack.
- To validate the study, the key metrics of the optimized concrete are compared with recent concrete models.

The later part of this research is discussed as follows: The recent works on concrete with their problem statements are mentioned in the first section. A novel proposed methodology is mentioned in the 2nd section. The outcomes and their discussions of the suggested model and comparisons are represented in the 3rd section. The 4th section concludes the study with subsequent works.

## MATERIALS AND METHODS

The present work aims to implement a novel termite-based Taguchi optimization (TbTO) to optimize the concrete mix. The main aim of adopting this technique is to improve the concrete quality without altering the quantity. Initially, the material parameters of the concrete are assigned to the perpendicular array of the system. After that, the material parameters based on major, minor, and intermediate terms are assigned in the novel approach to determine the optimized mix proportion in the concrete. Finally, the key metrics in the carbonation concrete are determined and correlated with recent concrete specimens, such as Fly Ash Concrete (FAC), Ordinary Portland Cement Concrete (OPCC) [33], and Residual Masonry concrete (RMC) [34]. The carbonation depth of the carbonation concrete is correlated with Carbonation concrete (CC) [35],

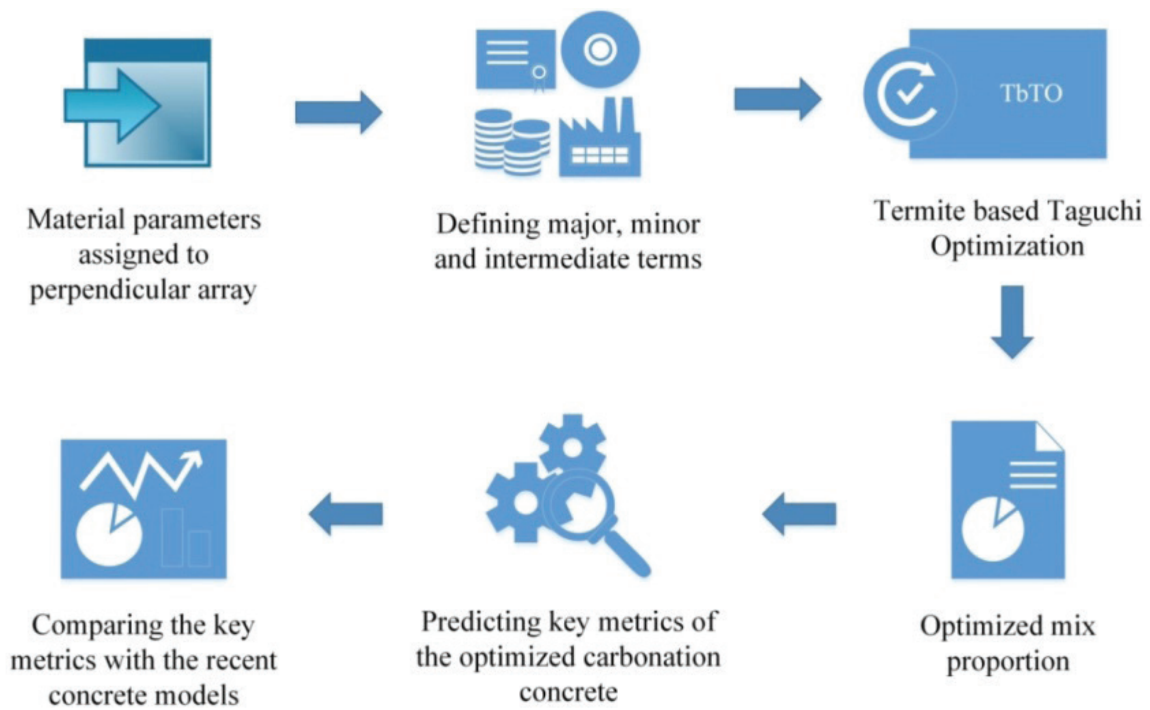


**Figure 1.** Proposed methodology.

Self Compacting Concrete by Masonry Residue (SCC-MR) [36], and Geopolymer Concrete (GPC) [37]. The chloride permeability of the carbonation concrete is correlated with Geopolymer concrete (GPC), Ordinary Portland Cement Concrete (OPCC) [37], and Fine Rice Husk Ash Concrete (FRHAC) [38]. The water Sorptivity of the carbonation concrete is correlated with Geopolymer Concrete (GPC) [34], Ordinary Portland Cement Concrete (OPCC), Fly Ash Concrete (FAC) and Silica Fume Concrete (SFC) [39]. The acid attack of the carbonation concrete is correlated with Geopolymer concrete (GPC) [40], Fly Ash Concrete (FAC), and Hybrid Fibre Concrete (HFC) [41]. All models were tested with the same proposed mix concentration from the same MATLAB software, and the results were compared. The reason for selecting these components is, which is the latest optimal technology executed by the different researchers.

The proposed methodology is illustrated in Figure 1. Initially, the material parameters of the concrete are assigned to the perpendicular array. Afterward, based on the major, minor, and intermediate input terms, these values are assigned to the novel TbTO. The output gained will be of optimized mix proportion. The key metrics of the concrete in terms of compression strength, carbonation depth, chloride permeability, sorptivity, and acid attack are determined. These key metrics are correlated with recent concrete models for validating the study.

**Materials**

Grade 40 ordinary Portland cement is implemented as the binder. 30% is the standard consistency of the cement used. 123 minutes is the initial setting time of the cement used, and 270 minutes is the final setting time of cement. 3.1 is the specific gravity of the cement, and 44.5 MPa is the compression strength of the cement used. Natural sand is considered fine aggregate, and its size is less than 4.75mm. 2.64 is the specific gravity of the cement. 0.87% is the water absorption capacity of the fine aggregate. 3.02 is the fineness modulus of the sand used. 10mm is the maximum size of the coarse aggregate, and 3.06 is the specific gravity of the coarse aggregate. 2.04% is the water-absorbing capacity of the coarse aggregate. 2.64 is the modulus of fineness in the coarse aggregate.

GGBS is a byproduct obtained from the steel and iron industry. GGBS reacts with water and cement during hydration and forms additional C-S-H gel and $Ca(OH)_2$. This additional chemical compounds increase the strength of concrete. For these advantages, GGBS is considered for this research. 3.1 is the specific gravity of the GGBS used in this research, and the fineness modulus of the GGBS is 12000 $cm^2/g$, 680 $kg/m^3$ is the bulk density of GGBS, and 27 sec is the marsh cone flow value of GGBS. The GGBS particle distribution of $d_{10}$, $d_{50}$, and $d_{90}$ are 1.5μm, 4.2 μm and 9μm. Silica fume also enhances the strength of concrete by forming $Ca(OH)_2$ and C-S-H gel. Silica fume is a byproduct obtained from the quartz manufacturing process. The residue of silica fume in the 90μm sieve is 4%.

**Mix Proportions**

The concrete grade executed in the work was M30 as per IS10262-2019. 0%, 20%, 40%, and 60% by weight of cement, the GGBS is replaced partially. The compression strength increased at the silica fume of 15% and decreased at the 20% replacement level. At this point, free Ca(OH)2 and silica utilization are at an optimum level [42]. Hence, 15% of silica fume is considered the optimum dosage level. Already, 15% SF has been researched, but it has reported dry density and poor compression strength [43]. To address these issues 15% of SF is considered for this study. The mix parameters and their values are represented in Table 2.

The sustainable concrete materials are then replaced in place of cement, and the mix proportions of the M30 concrete grade in terms of cement, water, silica fume, GGBS, fine aggregate, and coarse aggregate are represented in Table 3.

**Table 2.** Mix parameters and their values as per IS 10262 2019

| Mix parameters | Values |
|---|---|
| Target strength | 38.25 MPa |
| Water by cement ratio | 0.43 |
| Water content | 169.77 $kg/m^3$ |
| Cement content | 394.813 $kg/m^3$ |
| Air voids | 0.015 |
| Aggregate percentage in consideration with overall concrete | 68.633% |
| Coarse aggregate percentage in consideration with overall aggregate | 62% |
| Fine aggregate percentage in consideration with overall aggregate | 38% |
| Coarse aggregate content | 1302.105 $kg/m^3$ |
| Fine aggregate content | 688.526 $kg/m^3$ |
| Mix proportion | 1:1.74:3.3 |

**Table 3.** Mix proportions of M30 concrete mixes

| Mix proportions | Water (liter/m³) | Cement (kg/m³) | GGBS (kg/m³) | Silica fume (kg/m³) | Fine aggregate (kg/m³) | Coarse aggregate (kg/m³) |
|---|---|---|---|---|---|---|
| 0% SF, 0% GGBS | 169.77 | 394.813 | 0 | 0 | 688.526 | 1302.105 |
| 15% SF, 20% GGBS | 169.77 | 256.633 | 78.96 | 59.22 | 688.526 | 1302.105 |
| 15% SF, 40% GGBS | 169.77 | 177.633 | 157.93 | 59.22 | 688.526 | 1302.105 |
| 15% SF, 60% GGBS | 169.77 | 98.703 | 236.89 | 59.22 | 688.526 | 1302.105 |

**Mixing Preparation and Curing**

Based on the mix proportion, the samples are weight-batched, and the materials are placed in the tray. Initially, the coarse aggregate is placed, followed by the fine aggregate, then the fines are placed above the aggregates and the materials undergo dry mixing for 3 minutes. After that, water is added to the dry mix, and the wet mix is carried out. Once the concrete attains a uniform color, the fresh concrete is subjected to a slump cone test. On reaching the true slump, the concrete is placed in the molds with consideration to compaction in three layers. The molds are demoulded after 24 hours, and the specimens are placed in water curing for the particular days of curing. The chemical composition is defined in Table 4, physical composition is exposed in Table 5, and particle size distribution is in Table 6.

**Termite based Taguchi Optimization**

The Termite-based Taguchi optimization is designed with the functions of termite optimization and taguchi method. This dual model optimization is intended to improve the material quality without altering quantity. Hence, it is a novel approach to concrete technology. First, the material and strength parameters of the carbonation concrete from the experimental data are defined in the perpendicular array of the proposed approach, as expressed in Eqn. (1).

**Table 4.** Chemical composition

| Material | $SiO_2$ | $Al_2O_3$ | Fe2O3 | CaO | MgO | $SO_3$ | $Na_2O$ | $K_2O$ |
|---|---|---|---|---|---|---|---|---|
| Cement | 20.67 | 4.86 | 2.87 | 60.69 | 1.6 | 2.34 | 0.27 | 0.54 |
| GGBS | 38.94 | 11.16 | 1.94 | 30.75 | 7.65 | - | 1.4 | 0.26 |
| Silica Fume | 90.87 | 0.41 | 1.12 | 0.35 | 0.57 | 0.13 | 0.42 | 1.21 |

**Table 5.** Physical composition

| Material | Specific gravity | Bulk density | Particle size | Surface area (BET) |
|---|---|---|---|---|
| Cement | 3.12 | 1440 kg/m³ | <90µm | 232 m²/kg |
| GGBS | 2.74 | 1260 kg/m³ | <10µm | 600 m²/kg |
| Silica fume | 2.24 | 720 kg/m³ | <1µm | 12500 m²/kg |

**Table 6.** Particle size distribution & physical properties of aggregates

| Property | Fine aggregate | Coarse aggregate |
|---|---|---|
| Fineness modulus | 3.24 | 8.4 |
| Specific gravity | 2.62 | 2.67 |
| Absorption of water | 1.2% | 0.8% |
| Shape of particles | Rounded | Angular |
| Crushing value | - | 19.4 |
| Impact value | - | 12.14 |

$$P_a = \begin{cases} a_1, b_1, c_1, \ldots\ldots \\ a_2, b_2, c_2, \ldots\ldots \\ a_3, b_3, c_3, \ldots\ldots \\ a_m, b_m, c_m, \ldots\ldots \end{cases} \quad (1)$$

Where $a_1$, $a_2$, $a_3$, .... defines the parameter of concrete in the same category and $a_1$, $b_1$, $c_1$, .... defines the different parameters perpendicularly. Afterward, every parameter in the perpendicular array is assigned to the indication to dissonance ratio ($I / D$) for determining the minor, major, and intermediate terms shown in Eqn. (2), Eqn. (3), and Eqn. (4).

$$I / D_{\min or} = -10.1 \log_{10}\left(\frac{1}{m}\sum_{y=1}^{m} P^2\right) \quad (2)$$

$$I / D_{major} = -10.1 \log_{10}\left(\frac{1}{m}\sum_{y=1}^{m} \frac{1}{P^2}\right) \quad (3)$$

$$I / D_{\text{int}ermediate} = -10.1 \log_{10}\left(\frac{1}{m}\sum_{y=1}^{m} (P-R)^2\right) \quad (4)$$

Where $P$ defines the enhanced response in the system for the particular parameter and $R$ represents the average response of the specified parameter. The $I / D$ for each perpendicular array parameter is taken as an input in the optimization by the fitness function based on the quality characteristics. Major quality is considered for strength parameters, and minor quality is considered for voids in the concrete. Based on such conditions, an optimal mix proportion of concrete is obtained in the proposed approach. Once the mix proportion is obtained, the concrete mix proportion is trained in the carbon curing process for a definite period by the fitness function. The optimization's prediction function is initiated to determine the durability parameters as represented in Eqn. (5).

$$D_p = \begin{cases} [C_s]_{1,3,28,56} \\ [C_p, W_s]_{3,28} \\ [C_d, A_a]_{28,56} \end{cases} \quad (5)$$

Where $C_s$ are the compression strength and carbonation depth of the concrete at 1, 3, 28, and 56 days, $C_p$, $W_s$ are the chloride permeability and water sorptivity at 3 and 28 days. $A_a$, $C_d$ is the acid attack residual strength at 28 and 56 days.

**Algorithm 1: TbTO**

**Start**
{
**initialization()**
{
int $P_a$;
//assigning the material parameters

$$P_a = \begin{cases} a_1, b_1, c_1, \ldots\ldots \\ a_2, b_2, c_2, \ldots\ldots \\ a_3, b_3, c_3, \ldots\ldots \\ a_m, b_m, c_m, \ldots\ldots \end{cases}$$

}
**quality parameters()**
{
int $I / D_{\min or}, I / D_{major}, I / D_{\text{int}ermediate}$;
//fixing the enhanced response for material parameter

$$I / D_{\min or} = -10.1 \log_{10}\left(\frac{1}{m}\sum_{y=1}^{m} P^2\right)$$

$$I / D_{major} = -10.1 \log_{10}\left(\frac{1}{m}\sum_{y=1}^{m} \frac{1}{P^2}\right)$$

$$I / D_{\text{int}ermediate} = -10.1 \log_{10}\left(\frac{1}{m}\sum_{y=1}^{m} (P-R)^2\right)$$

//determining I/D
}
**testing()**
{
int $D_p$;
//initializing durability parameters

$$D_p = \begin{cases} [C_s]_{1,3,28,56} \\ [C_p, W_s]_{3,28} \\ [C_d, A_a]_{28,56} \end{cases}$$

//finalizing parameters
}
}
**End**

Initially, the material parameters of the carbonation concrete are assigned to the perpendicular array. Afterward, based on the quality of parameters, they are defined according to the proposed approach in major, minor, and intermediate responses. From the proposed approach the optimized concrete mix proportion is obtained. Subsequently, the carbon curing is carried out in the samples. The key metrics of the concrete in terms of compression strength, carbonation depth, chloride permeability, sorptivity, and acid attack are determined and correlated with the recent concrete models for validating the study. Precisely, by implementing the above steps, accurate outcomes can be obtained.

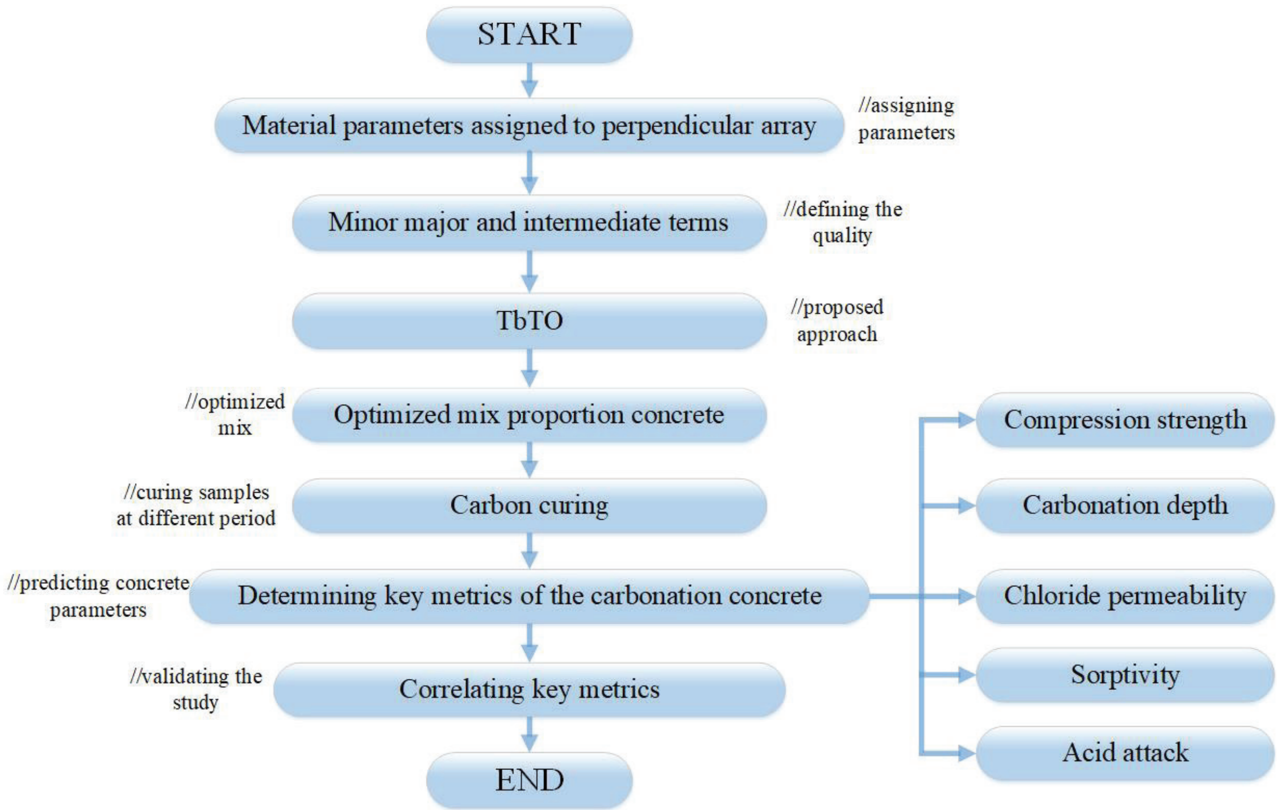


**Figure 2.** Flow process of the proposed approach.

## RESULTS AND DISCUSSION

The proposed technique is executed in the Windows 10 Operating System. The process is carried out in MATLAB R2023a Windows software. The Matrix Laboratory is the full form of MATLAB, computer software for data analysis, algorithm development, and models and applications. It has multi-layers of programming that have operational and functional direction points. It is generally utilized by mathematicians and research scholars to develop complex models in programming. This software is also employed to predict numerical data and perform graphical visualizations. Numerical computations, intelligent data learning and prediction, and data processing in academic studies are the applications of this software. The TbTO approach is developed in MATLAB to determine the optimal mix proportion from the material properties. Thereafter, the optimal mix proportion is trained in the carbon curing process, and the durability parameters are predicted and correlated with the recent concrete studies.

### Case Study

To validate the proposed approach, the tests on the carbonation concrete are carried out, and the outcomes are illustrated in order. The tests include compression strength, carbonation depth, chloride permeability, water sorptivity, and acid attack. The specimen size and curing period will also vary for each test. The curing is carried out only by the carbon curing process. The compression strength of the sample is 10×10×10 cm, and the testing is carried out for 1,3,28 and 56 days. The carbonation depth is calculated on 28 and 56 days. The water sorptivity is determined in the concrete specimen with a length of 50 mm and a diameter of 100mm. The chloride permeability in the concrete specimen has dimensions of 50 mm length and 100 mm diameter. The chloride permeability and the water sorptivity tests are carried out in 3 days and 28 days of carbon curing. The acid attack was carried out in a sample size of 10×10×10 cm, and the testing was carried out on $28^{th}$ and $56^{th}$ day. The procedure for testing and their results are represented in sequence and order.

The precision in the proposed approach was defined by correlating the outcomes with the recent concrete studies, which included compression strength, carbonation depth, water sorptivity, chloride permeability, and acid attack. For comparison, the carbonation depth, acid attack, and compression strength of the $28^{th}$ and $56^{th}$ day results are taken, and for chloride permeability and water sorptivity, $28^{th}$ day results are considered. The carbonation concrete with 15% silica fume and 40% GGBS has shown better compression strength and acid attack results. The mix with a higher amount of admixture has lower permeability, that is the mix with 15% silica fume and 60% GGBS. This mix proportion possesses lower carbonation depth, water sorptivity, and chloride permeability.

The mix containing 15% silica fume and 60% GGBS is considered for its superior strength behavior and optimum permeability. The carbonation concrete by the proposed approach is carried out using MATLAB R2021 software with precise specimen sizes and carbon curing conditions to obtain accurate outcomes. Thereafter the outcomes are compared with recent concrete investigations for validating the research. The concrete references used in the comparisons correlate with their material composition, as shown in Table 7.

**Compression Strength**

The compression strength of concrete on the 28th day defines the grade of concrete. It is expressed in load per area. The ability of the specified dimension cube based on the size of coarse aggregate to resist the compression load without yielding is termed the compression strength of the cube. The compression strength tests are determined in cubes of size 100 × 100 × 100 mm, and the tests are carried out in 1, 3, 28, and 56 days. The load is considered to be applied on the cube's right angle to the concrete placing side as per BIS 516-1959. The rate of loading is 2.4 MPa per second. The compression strength of the carbonation concrete at 1,3,28 and 56 days of curing are represented in Figure 3.

The compression value of the carbonation concrete at 1 day of testing was 5 MPa for the conventional mix. The silica fume is fixed for the mixes at 15%. The mix containing 20% GGBS has a compression value of 5.2 MPa, 40% GGBS has a compression strength of 5.7 MPa, and 60% has a compressive strength of 5.4 MPa. On 3rd day of testing, the conventional mix had a compression value of 10 MPa, the mix having 20% GGBS had a compression value of 10.3 MPa, the mix having 40% GGBS had a compressive value of 11.11 MPa, and the mix containing 60% GGBS has a compressive strength of 11 MPa.

On the 28th day of testing the conventional mix had a compression strength value of 40 MPa, the mix having 20%

**Table 7.** Comparison of different types of concrete with their material composition

| Concrete | Cement (Kg/m³) | Water (l/m³) | Fine aggregate (Kg/m³) | Coarse aggregate (Kg/m³) | Sustainable material | Replacement material | Replacement material (Kg/m³) |
|---|---|---|---|---|---|---|---|
| Fly Ash Concrete (FAC) [33] | 286 | 165 | 1007 | 883 | Fly ash | cement | 72 |
| Ordinary Portland Cement Concrete (OPCC) [33] | 358 | 165 | 1007 | 883 | - | - | - |
| Residual Masonry concrete (RMC) [34] | 375 | 202.5 | 895.11 | 686.21 | Masonry residue | cement | 106.4 |
| Self-Compacting Concrete by Masonry Residue (SCC-MR) [34] | 375 | 202.5 | 895.11 | 686.21 | Masonry residue | cement | 106.4 |
| Carbonation concrete (CC) [35] | 330 | 198 | 719 | 813 | Carbonation curing | - | - |
| Geopolymer Concrete (GPC) [37] | - | 263 (Alkali activate slag) | 685 | 1058 | GGBS and MBS | cement | 364.5 and 40.5 |
| Fine Rice Husk Ash Concrete (FRHAC) [38] | 40 | 180 (Alkali activate slag) | 576 | 1070 | Fine rice husk ash | cement | 360 |
| Ordinary Portland Cement Concrete (OPCC) [39] | 550 | 192.5 | 989.5 | 662.5 | - | - | - |
| Fly Ash Concrete (FAC) [39] | 385 | 192.5 | 922.5 | 615 | Fly ash | cement | 165 |
| Silica Fume Concrete (SFC) [39] | 495 | 192.5 | 975 | 652.5 | Silica fume | cement | 55 |
| Geopolymer concrete (GPC) [40] | - | 141.75 | 683 | 1269 | Fly ash and GGBS | cement | 303.75 and 101.25 |

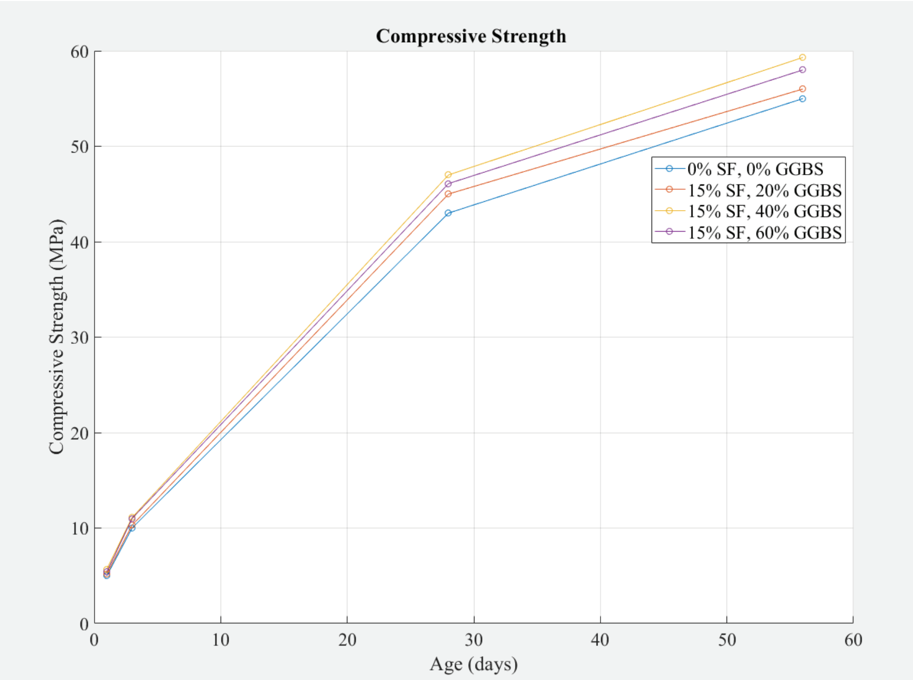


**Figure 3.** Compression strength of carbonation concrete at 1,3,28 and 56 days of testing.

**Table 8.** Compression strength of carbonation concrete at 1, 3, 28, and 56 days of testing

| Proportions | Compressive strength (MPa) | | | | Error bar |
|---|---|---|---|---|---|
| | 1 day | 3 days | 28 days | 56 days | ±4 |
| 0% SF 0% GGBS | 5 | 10 | 43 | 55 | ±6 |
| 15% SF 20% GGBS | 5.2 | 10.3 | 45 | 56 | ±3 |
| 15% SF 40% GGBS | 5.7 | 11.11 | 47 | 59.31 | ±1 |
| 15% SF 60% GGBS | 5.4 | 11 | 46.09 | 58 | ±2 |

GGBS had a compression strength value of 45 MPa, the mix containing 40% GGBS had a compression strength value of 47 MPa, and the mix containing 60% GGBS has compression strength of 46.09 MPa. On the 56$^{th}$ day in the compression strength testing, the conventional concrete had a compressive strength value of 55 MPa, the mix containing 20% GGBS had a compression strength value of 56 MPa, the mix having 40% GGBS had a compressive strength value of 59.31 MPa and the mix having 60% GGBS has compressive strength value of 58 MPa. The compression strength of the carbonation concrete at 1, 3, 28, and 56 days, along with various mix ratios, are represented in Table 8. Compared with all these tests, the mix containing 15% silica fume (SF) and 40% GGBS has higher compression strength than all the other mix proportions.

The strength of compression in the concrete was represented in MPa. The compression strength in the carbonation concrete on the 28$^{th}$ day and 56$^{th}$ day are compared with FAC, OPCC [33], and RMC [34]. On the 28$^{th}$ day, the strength of compression in the FAC is 32 MPa, the OPCC has the strength of compression of 37 MPa, and the RMC has the strength of compression of 38 MPa.

The proposed approach carbonation concrete has compression strength of 47 MPa at the 28$^{th}$-day test. The graphical representation of the compression strength in the carbonation concrete on the 28$^{th}$-day and 56$^{th}$-day results is represented in graphical format in Figure 4 and Table 9. At the 56$^{th}$ day test, the FAC's compression strength is 48 MPa, the OPCC has the strength of compression as 52 MPa [33], and the RMC has a compressive strength of 47 MPa [34].

The proposed approach to carbonation concrete has compression strength of 59.31 MPa. The compression strength outcomes show that carbon curing concrete possesses higher strength than admixture replacement concretes and ordinary concrete.

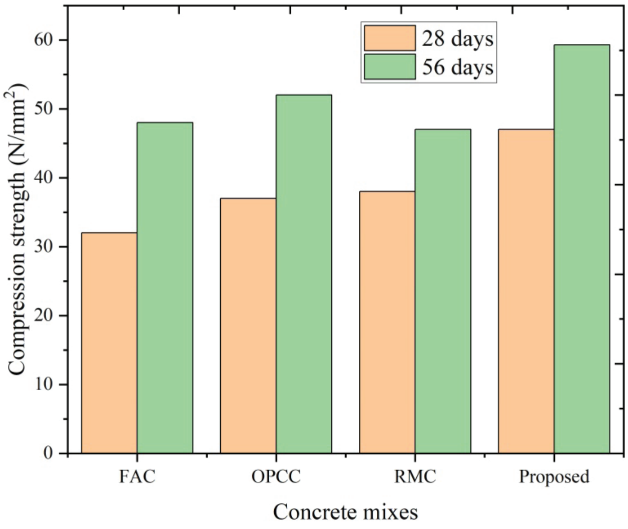


**Figure 4.** Comparison of compression strength in the proposed concrete with the recent concrete models.

**Carbonation Depth**

The $CO_2$ from the environment reacts with the hydration particles of the concrete and forms carbonate, leading to steel bar corrosion. Thus, the strength properties of concrete structures are altered. The depth at which the carbon particles penetrate inside the concrete member from the extreme fiber of concrete is termed carbonation depth. The depth of carbonation in the carbon-cured concrete is represented in graphical format in Figure 5.

On the 28th day, the depth of carbonation in the concrete is 4mm for the conventional mix, the mix with 20% GGBS has a carbonation depth of 5mm, the mix with 40% GGBS has a carbonation depth of 4mm, and the 60% GGBS mix has carbonation depth of 3mm. The statics of the carbonation depth of the carbonation concrete at the 28 days and 56 days of testing are illustrated in Table 10 and Figure 5.

On the 56th day of testing the conventional concrete had a depth of carbonation of 8mm, the concrete having 20% GGBS had a depth of carbonation of 9mm, the concrete

**Table 9.** Comparison of compression strength in the proposed concrete along with the recent concrete models

| Testing day | Compression strength (MPa) | | | |
|---|---|---|---|---|
| | **FAC** | **OPCC** | **RMC** | **Proposed** |
| 28th day | 32 | 37 | 38 | 47 |
| 56th day | 48 | 52 | 47 | 59.31 |

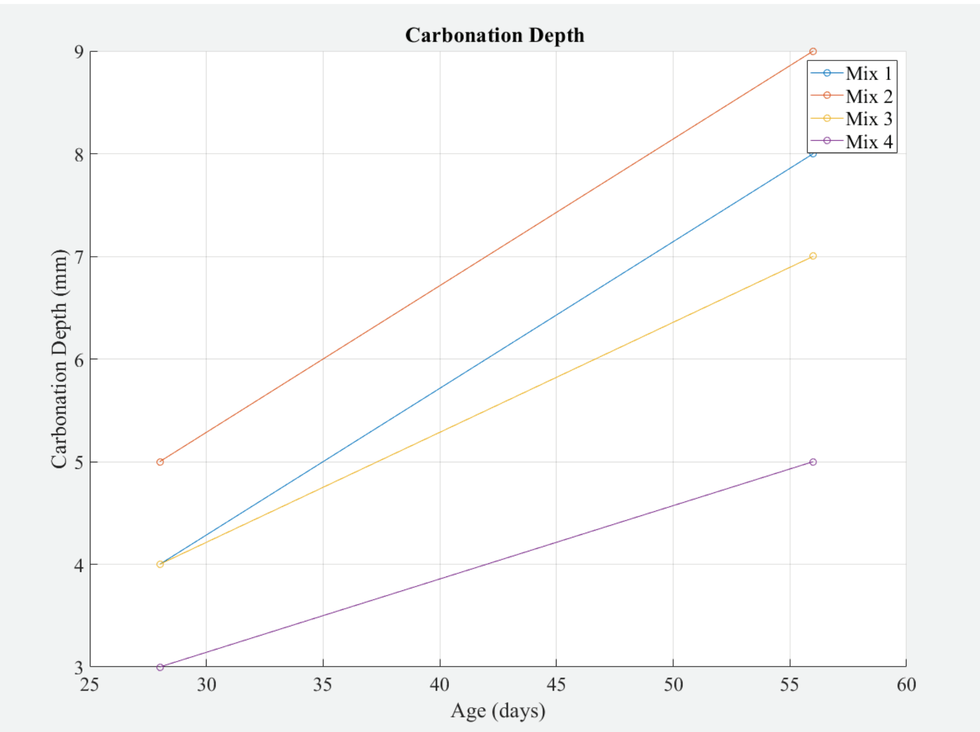


**Figure 5.** Carbonation depth of carbonation concrete at 28 and 56 days of testing.

**Table 10.** Carbonation depth of carbonated concrete at 28 and 56 days of testing

| Proportions | Carbonation depth (mm) | |
|---|---|---|
| | 28 days | 56 days |
| 0% SF 0% GGBS | 4 | 8 |
| 15% SF 20% GGBS | 5 | 9 |
| 15% SF 40% GGBS | 4 | 7 |
| 15% SF 60% GGBS | 3 | 5 |

having 40% GGBS had a depth of carbonation of 7mm, and the concrete having 60% GGBS has carbonation depth of 5mm. The mix containing 15% SF and 60% GGBS has a lower carbonation depth than the other mix proportions. The mineral admixture silica fume and GGBS will minimize the permeability in concrete, resulting in reduced carbonation depth in the admixture concrete.

The depth of carbonation in the concrete was represented in mm. The depth of carbonation in the proposed concrete was correlated with CC [35], SCC-MR [36], and GPC [37]. The carbonation depth in the suggested model is compared with the conventional carbonation concrete, eco-friendly self-compaction concrete, because the residual wastes in the environment are reduced in the form of concrete, and the full cement is replaced by admixture concrete, which is the GPC. The comparison statics of the carbonation depth of various concrete mixes with the suggested concrete are represented in Figure 6 and Table 11.

On the 28th day, the depth of carbonation in the existing carbonation concrete was 16.5 mm, the SCC-MR had a carbonation depth of 5 mm, and the GPC had a carbonation depth of 8.55 mm. The proposed carbonation concrete has a carbonation depth of 4mm.

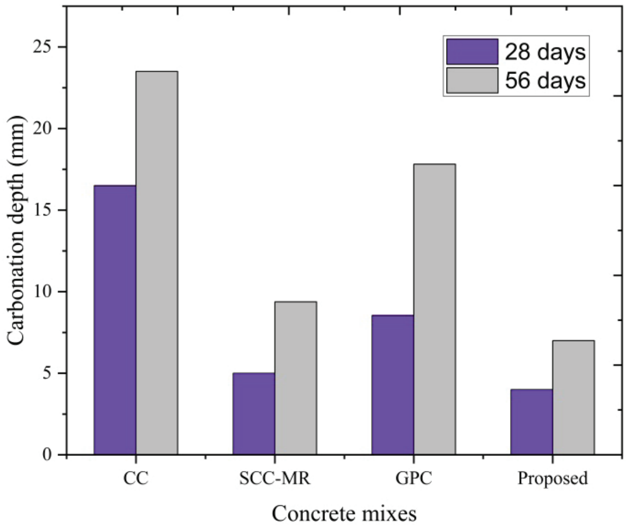


**Figure 6.** Comparison of carbonation depth of the proposed concrete with the recent concrete models.

**Chloride Permeability**

The permeability of chloride in the concrete defines the durability of the concrete at various exposure conditions. The ingression of chloride ions in concrete directly impacts its endurance. The chloride penetration in the concrete is expressed in terms of electrical conductance, which is concrete resistance to chloride ion penetration. The specimen size for the permeability test in chloride is a diameter of 100 mm and a height of 50 mm cylindrical specimen. The samples were tested on 3 and 28 days concerning ASTM 1202. One end of the sample is considered to be associated with the solution of sodium hydroxide, and the other end is associated with the solution of sodium chloride. The samples are tested for 6 hours. The potential difference maintained is 60V.

On 3rd day of testing the chloride permeability of the conventional concrete was 4276.28 coulombs, the mix containing GGBS of 20% had a chloride permeability of 3018.71 coulombs, the mix containing 40% GGBS had a chloride permeability of 1238.41 coulombs and the mix containing 60% GGBS has chloride permeability of 689.68 coulombs. The statistics of the chloride permeability test on the 3rd and the 28th day are represented in Table 12 and Figure 7. After curing for 28 days, the chloride permeability was reduced [44].

At the 56th day test the conventional mix has a chloride permeability of 2138.14 coulombs, the mix having 20% GGBS has a permeability by chloride of 1509.36 coulombs, the mix having 40% GGBS has a permeability of chloride as 619.21 coulombs. The mix with 60% GGBS has a chloride permeability of 344.84 coulombs. The mix containing 15% SF and 60% GGBS has lower chloride permeability than the other mix proportions because these mix proportions possess a higher admixture percentage than all the other

**Table 11.** Correlation in carbonation depth of the proposed concrete with the recent concrete models

| Testing day | Carbonation depth (mm) | | | |
|---|---|---|---|---|
| | CC | SCC-MR | GPC | Proposed |
| 28th day | 16.5 | 5 | 8.55 | 4 |
| 56th day | 23.5 | 9.38 | 17.82 | 7 |

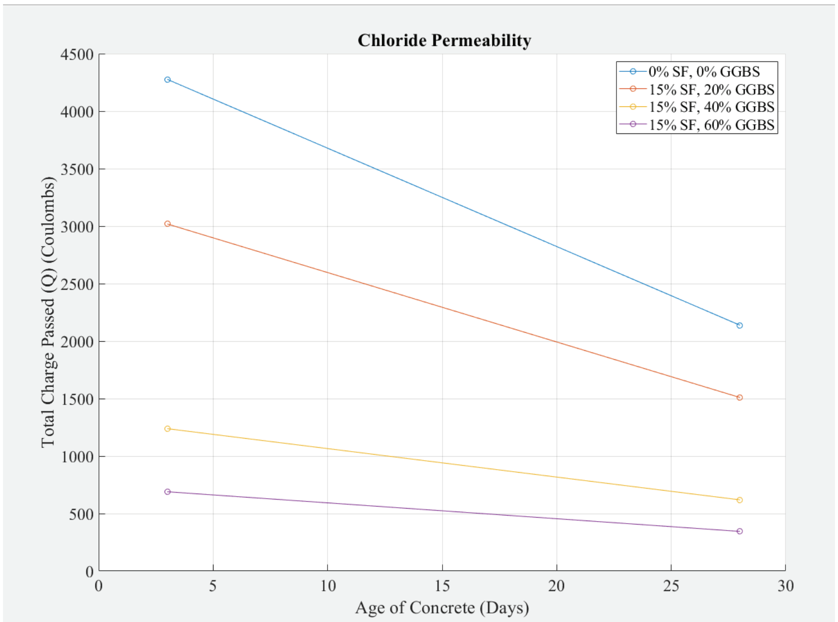


**Figure 7.** Chloride permeability of carbonation concrete at 3 and 28 days of testing.

**Table 12.** Chloride permeability of carbonation concrete at 3 and 28 days of testing

| Proportions | Chloride permeability (Coulombs) | |
|---|---|---|
| | 3 days | 28 days |
| 0% SF 0% GGBS | 4276.28 | 2138.14 |
| 15% SF 20% GGBS | 3018.71 | 1509.36 |
| 15% SF 40% GGBS | 1238.41 | 619.21 |
| 15% SF 60% GGBS | 689.68 | 344.84 |

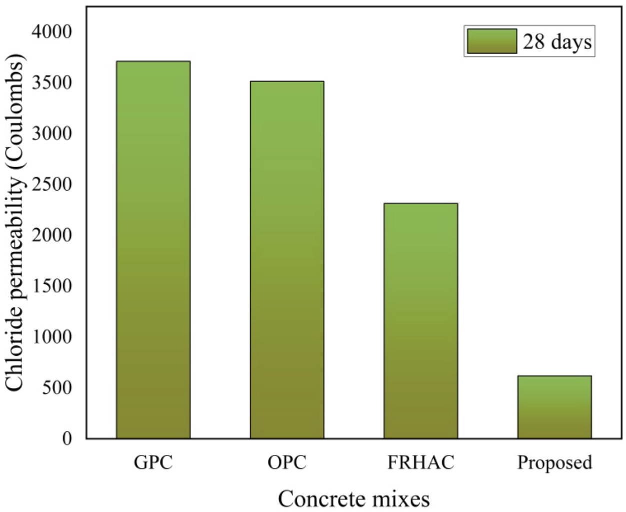


**Figure 8.** Comparison of chloride permeability of the proposed concrete with the recent concrete models.

mixes.All concrete mix mixtures saw a significant decrease in chloride permeability from 3 to 28 days since once the concrete cures, the cement particles keep continuing to hydrate, creating a dense microstructure using fewer overlapping pores that prevents chloride ions compared to permeating the concrete matrix.

The permeability of chloride ions in the concrete is represented in coulombs. The chloride permeability of the proposed carbonation concrete is correlated with GPC, OPCC [37], and FRHAC [38]. The OPCC is the traditional concrete, and GPC is the concrete where other admixtures replace the binder cement. The FRHAC concrete is made with fine rice husk with cement's partial replacement. The correlation of the permeability by the chloride ions of the carbonation concrete is illustrated in Figure 8 and Table 13. On the 28$^{th}$ day, the chloride permeability of GPC is 3712 coulombs. The OPCC has a chloride permeability of 3515 coulombs, and the FRHAC has a chloride permeability of 2314 coulombs. The proposed approach has a chloride permeability of 619.21 coulombs.

**Table 13.** Comparison of chloride permeability tests

| Concrete | 28$^{th}$-day Chloride permeability (Coulombs) |
|---|---|
| GPC | 3712 |
| OPCC | 3515 |
| FRHAC | 2314 |
| Proposed | 619.21 |

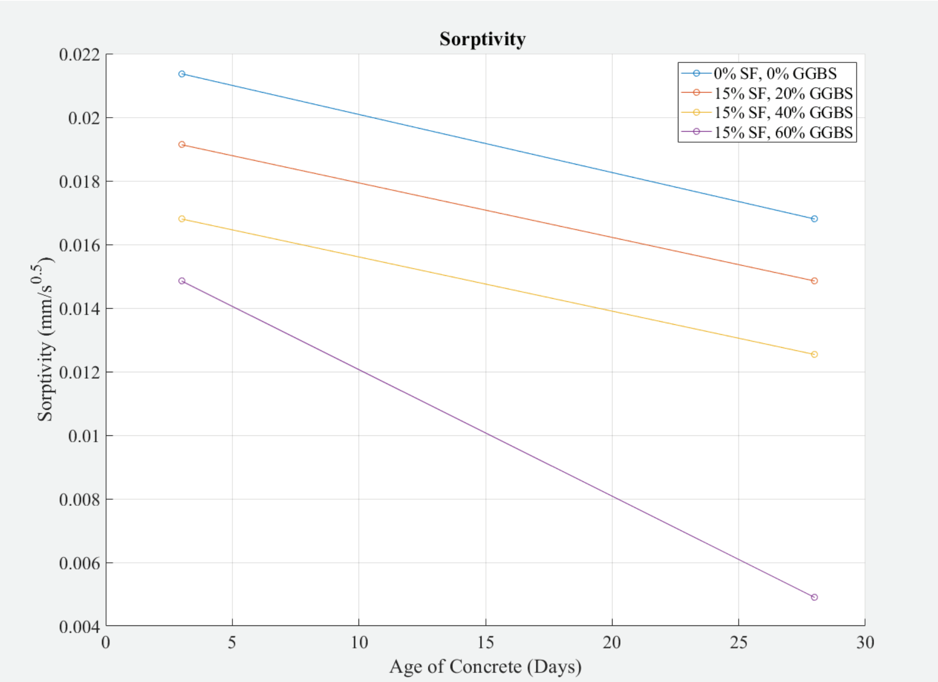


**Figure 9.** Water sorptivity of carbonation concrete at 3 and 28 days of testing.

**Sorptivity**

Sorptivity defines the concrete's ability to absorb and transmit water in the pore structure of concrete by the action of capillarity. The sorptivity test is conducted on 3 and 28 days as per ASTM C 1585 – 04. The specimen for testing is a cylinder with 100 mm diameter and 50 mm length. The curved surface in the specimen is considered to be coated with epoxy resin. The water level is kept 2-3 mm above the supporting frame. The test outcomes of the water sorptivity at 3 days and 28 days of carbon curing are represented in Figure 9 and Table 14.

On the 3$^{rd}$ day of testing the conventional mix had a water sorptivity of 0.0214 mm/s$^{0.5}$, the mix with 20% GGBS had a water sorptivity of 0.0191 mm/s$^{0.5}$, the mix with 40% GGBS had a water sorptivity of 0.0168 mm/s$^{0.5}$, and the mix with 60% GGBS has water sorptivity of 0.0149 mm/s$^{0.5}$. The statistics of the water sorptivity of the proposed carbonation concrete at 3 days and 28 days of testing are represented in Table 14.

**Table 14.** Water sorptivity of carbonation concrete at 3 and 28 days of testing

| Proportions | Water sorptivity (mm/s$^{0.5}$) | |
|---|---|---|
| | 3 days | 28 days |
| 0% SF 0% GGBS | 0.0214 | 0.0168 |
| 15% SF 20% GGBS | 0.0191 | 0.0149 |
| 15% SF 40% GGBS | 0.0168 | 0.0125 |
| 15% SF 60% GGBS | 0.0149 | 0.0049 |

On the 28$^{th}$ day, the water sorptivity of the conventional carbonation concrete is 0.0168 mm/s$^{0.5}$, the mix containing 20% GGBS has water sorptivity of 0.0149 mm/s$^{0.5}$, the mix containing 40% GGBS has water sorptivity of 0.0125 mm/s$^{0.5}$ and the mix containing 60% GGBS has water sorptivity of 0.0049 mm/s$^{0.5}$. The mix with 15% SF and 60% GGBS has lower water sorptivity than the other mixes. Due to the reason, that the mix with more amount of silica fumes and GGBS has lower water sorptivity due to the reason that rise in the admixture percentage of the concrete increases the permeability in concrete and reduces the water sorptivity.

The water sorptivity in the concrete was determined in terms of mm-sec$^{0.5.}$ The water sorptivity of the carbonation concrete is correlated with GPC [34], OPCC, SFC, and FAC [39]. The water sorptivity in the proposed concrete is correlated with the recent concrete models and is represented in Figure 10.

On the 28$^{th}$ day, the GPC has a water sorptivity of 0.0243 mm-sec$^{0.5}$, the OPCC has a water sorptivity of 0.0253 mm-sec$^{0.5}$, the SFC has a water sorptivity of 0.075 mm-sec$^{0.5}$ and the FAC has water sorptivity of 0.089 mm-sec$^{0.5}$. The proposed approach has a water sorptivity of 0.0125 mm-sec$^{0.5}$. The water sorptivity in the proposed concrete is correlated with the recent concrete model as represented in Table 15.

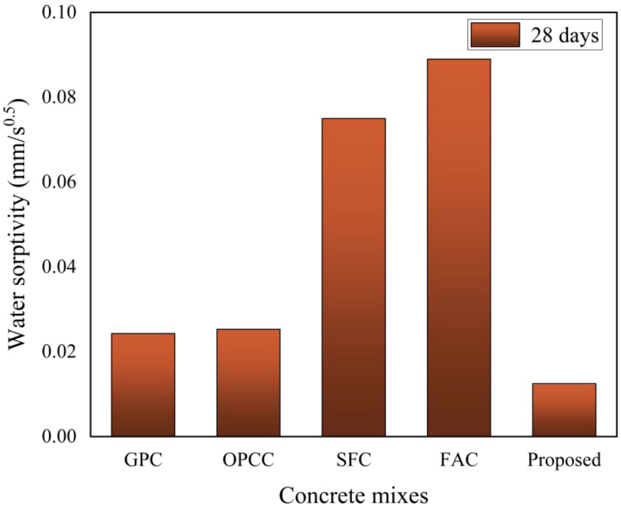


**Figure 10.** Correlation of water sorptivity in the proposed concrete with the recent concrete samples.

**Table 15.** Water sorptivity comparison of the proposed concrete with the recent models

| Concrete | 28$^{th}$-day water sorptivity (mm/sec$^{0.5}$) |
|---|---|
| GPC | 0.0243 |
| OPCC | 0.0253 |
| SFC | 0.075 |
| FAC | 0.089 |
| Proposed | 0.0125 |

**Acid Attack**

In chemically aggressive environments like sewage collection systems, concrete degradation occurs due to the presence of Hydrogen sulphide, moisture, and oxygen. Thus the design period of concrete structures is affected. An acid attack test is performed to determine the acid resistance in the concrete. The specimens in the acid attack test are of size 100 × 100 × 100 mm cube. Initially, for 10 days, the cubes are cured as usual. Afterward, the cubes are considered acid curing in a 2% sulphuric acid solution with pH maintained at 1 ± 0.1. Here, 0.1 is the fitness value adopted from the termite optimization. For the acid attack test, strength in compression of the acid-cured sample is tested at 28 and 56 days. The acid attack test outcome at 28 days and 56 days is represented in Figure 11.

Conventional carbonation concrete has a strength reduction of 9.98% on the 28$^{th}$ day of testing and an 18.04% strength reduction on the 56$^{th}$ day test. The mix containing 20% GGBS has a strength reduction of 8.73% on the 28$^{th}$ and 12.3% on the 56$^{th}$ day of testing. The mix containing 40% GGBS has a strength reduction of 6.26% on the 28$^{th}$ day of testing and a 10.93% strength reduction on the 56$^{th}$ day of testing. The mix containing 60% GGBS has a strength reduction of 7.27% on the 28$^{th}$ day of testing and a 14.53% strength reduction on the 56$^{th}$ day of testing. The statistics of the strength reduction in the acid attack test are represented in Table 16.

The mix containing 15% silica fume and 40% GGBS has a lower reduction in strength than the other models. This is because adding admixture in the proportions of concrete increases the concrete strength to an optimum level. After that, a reduction in strength occurs. Hence, compared with

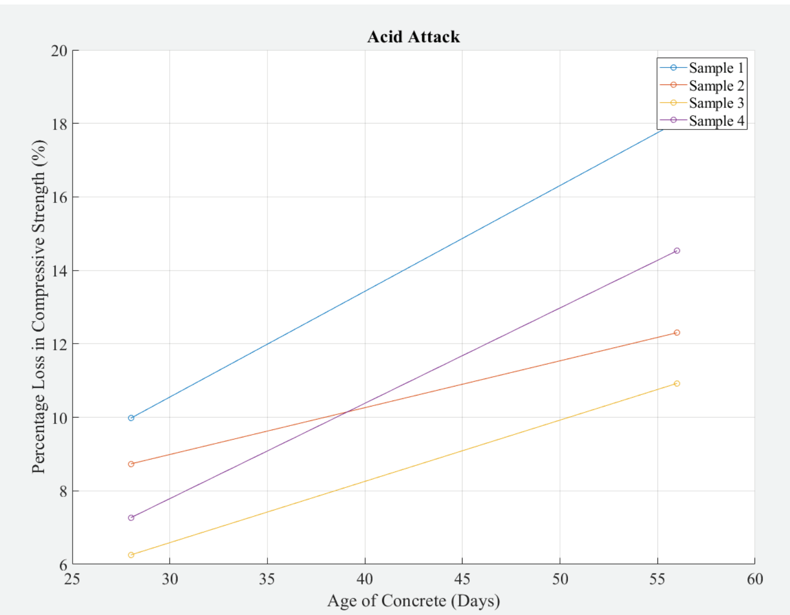


**Figure 11.** Percentage in strength loss of carbonation concrete at 28$^{th}$, and 56$^{th}$ days of acid curing.

**Table 16.** Acid attack in carbonation concrete on the 28th, and 56th days of testing

| Proportions | Reduction in strength (%) | |
|---|---|---|
| | 28 days | 56 days |
| 0% SF 0% GGBS | 9.98 | 18.04 |
| 15% SF 20% GGBS | 8.73 | 12.30 |
| 15% SF 40% GGBS | 6.26 | 10.93 |
| 15% SF 60% GGBS | 7.27 | 14.53 |

all other mix proportions, the mix proportion of 15% silica fume and 60% GGBS has a lower reduction in strength in the acid attack test.

In an acid attack test, the curing is carried out by implementing a percentage of acid per amount of water. Thus, the strength in curing specimens is lowered through the acid percentage. This strength in terms of percentage is the outcome of the acid attack test. At the 28-day curing period, the GPC has a strength reduction of 7.124%, the FAC has a strength reduction of 9.51%, and the HFC has a strength reduction of 9.82%. The proposed approach has a strength reduction of 6.26%. The comparison graph of the acid attack in the 28th-day tests and the 56th-day tests is shown in Figure 12 and Table 17.

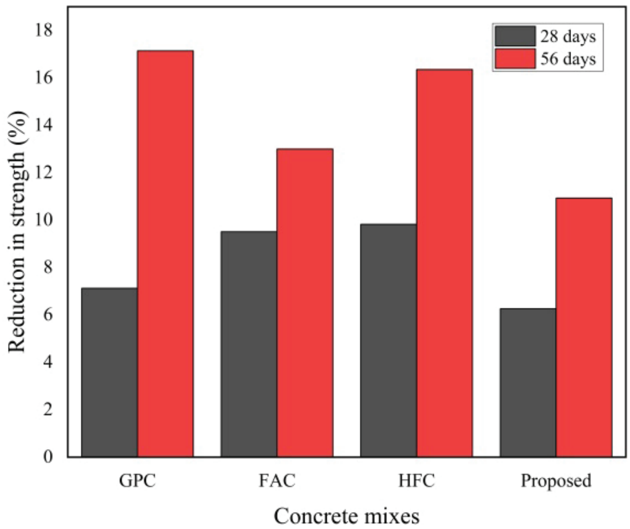


**Figure 12.** Comparison of the reduction in strength by acid attack of the proposed concrete with the recent concrete models.

**Table 17.** Comparison of acid attack test results

| Testing day | Reduction in strength (%) | | | |
|---|---|---|---|---|
| | GPC | FAC | HFC | Proposed |
| 28th day | 7.124 | 9.51 | 9.82 | 6.26 |
| 56th day | 17.14 | 13 | 16.35 | 10.93 |

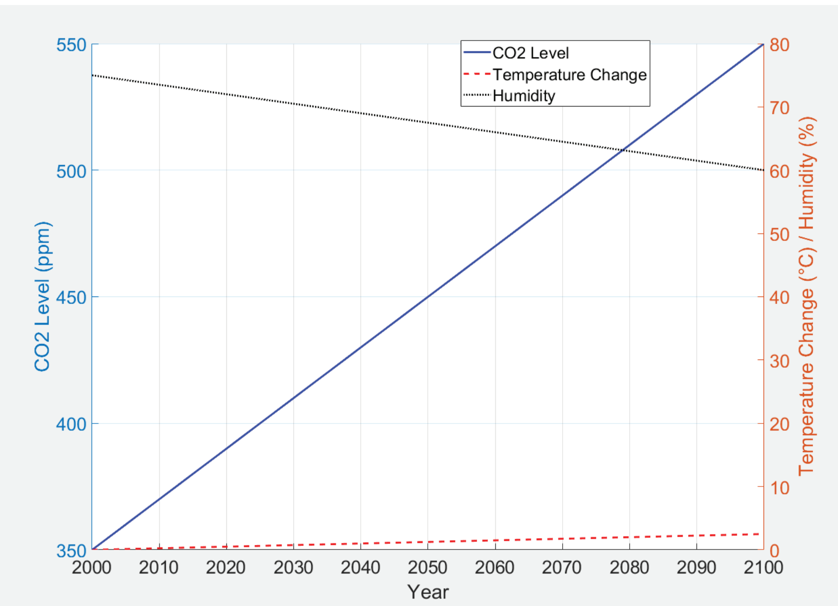


**Figure 13.** Environmental impact.

At the 56-day curing period, the GPC has a strength reduction of 17.14%, the FAC has a strength reduction of 13%, and the HFC has a strength reduction of 16.35%. The proposed approach has a strength reduction of 10.93%. The strength reduction is considered from the normal concrete strength.

The validated environmental impacts on three different parameters $Co_2$, temperature change, and humidity, are exposed in Figure 13.

## CONCLUSION

This research aimed to deliver a novel Termite-based Taguchi Optimization to determine the concrete mix ratio. Initially, the material parameters in the concrete are assigned in the system. Based on the major, minor, and intermediate terms, the assigned parameters are optimized using the novel approach, and an optimal mix proportion for M30 grade concrete is obtained. Thus, mixed proportion concrete undergoes a carbonation curing training process for the required periods in definite sample sizes monitored under the fitness function. Afterward, the prediction system in the optimization is triggered to determine the durability parameters of the concrete. The durability parameters are determined regarding compression strength, carbonation depth, water sorptivity, chloride permeability, and acid attack.

- The mix containing 15% silica fume and 40% GGBS is considered the optimum mix because it possesses high compression strength and acid attack values. The carbonation depth, water sorptivity, and the permeability of chloride ions in the mix are also at the optimum level.
- The compression strength of the proposed carbonation concrete is 47 MPa on the $28^{th}$ day test, which is 23.68% higher than other concrete, and on the $56^{th}$ day, the compression strength is 59.31MPa, which is 14.1% higher than other compared models.
- The carbonation depth of the proposed concrete is 4 mm on the $28^{th}$ day, which is 20 % lower than other compared models, and on the $56^{th}$ day, the carbonation depth is 7 mm which is 25% lower than other compared models.
- The chloride permeability of the proposed concrete was 619.21 coulombs at the 28th day test, which is 73.24% lower than that of other models.
- The water sorptivity of the proposed concrete was 0.0125 mm-sec0.5 on the 28th day test, which is 48.55% lower than that of the other models.
- The acid attack of the proposed concrete showed a 6.26% strength reduction at the 28th-day test, which is 0.864% lower than other compared models. On the $56^{th}$ day, the strength reduction was 10.93%, which is 2.07% lower than other compared models.

Considering the results, the proposed approach has considerably enhanced prediction ability with necessary features for building construction applications. Future studies in this section of concrete technology improve the process by including prediction accuracy, and behavior patterns of concrete, leading to the development of an accurate model in the upcoming days.

## NOMENCLATURE

| | |
|---|---|
| MPa | megapascal |
| sec | second |
| $CO_2$ | carbon dioxide |
| pH | Potential of hydrogen |
| mm | millimeter |
| $Ca(OH)_2$. | Calcium hyroxide |
| μm | Micrometer |
| $kg/m^3$ | Kilogram per meter cube |
| $cm^2/g$ | Centimeter square per gram |
| $SiO_2$ | Silicon dioxide |
| $Al_2O_3$ | Aluminium oxide |
| $Fe_2O_3$ | Ferric oxide |
| CaO | Calcium oxide |
| MgO | Magnesium oxide |
| $Na_2O$ | Sodium oxide |
| $K_2O$ | Potassium oxide |
| $SO_3$ | Sulfur trioxide |

## AUTHORSHIP CONTRIBUTIONS

Authors equally contributed to this work.

## DATA AVAILABILITY STATEMENT

The authors confirm that the data that supports the findings of this study are available within the article. Raw data that support the finding of this study are available from the corresponding author, upon reasonable request.

## CONFLICT OF INTEREST

The author declared no potential conflicts of interest with respect to the research, authorship, and/or publication of this article.

## ETHICS

There are no ethical issues with the publication of this manuscript.

## STATEMENT ON THE USE OF ARTIFICIAL INTELLIGENCE

Artificial intelligence was not used in the preparation of the article.

## REFERENCES

[1] Song W, Yang W, Wang N, Wang C, Li Z, Ou Y, et al. How does industrial transformative process shape the spatial dynamics of urban development? Land Use Policy 2024;138:107015. [CrossRef]

[2] Ahmed I, Mehrez K, Socci C, Deriu S, Mathkur NM, Casasr IP. Disaggregated effect of construction investments on the Saudi economy: a dynamic computable general equilibrium model of Saudi Arabia. Financ Innov 2024;10:28. [CrossRef]

[3] Chen L, Hu Y, Wang R, Li X, Chen Z, Hua J. Green building practices to integrate renewable energy in the construction sector: a review. Environ Chem Lett 2024;22:751–784. [CrossRef]

[4] Santos G, Esmizadeh E, Riahinezhad M. Recycling construction, renovation, and demolition plastic waste: review of the status quo, challenges and opportunities. J Polym Environ 2024;32:479–509. [CrossRef]

[5] Ahmed O, Ahmad S, Adekunle SK. Carbon dioxide sequestration in cementitious materials: a review of techniques, material performance, and environmental impact. J CO2 Util 2024;83:102812. [CrossRef]

[6] Karadumpa CS, Pancharathi RK. Study on energy use and carbon emission from manufacturing of OPC and blended cements in India. Environ Sci Pollut Res 2024;31:5364–5383. [CrossRef]

[7] Pontikes Y, Snellings R. Cementitious binders incorporating residues. In: Handbook of recycling. Elsevier; 2024:429–444. [CrossRef]

[8] Yang Y, Lu P, Shao R, Zhao Q, Yang T, Wu C. A comprehensive review of multisource solid wastes in sustainable concrete: from material properties to engineering application. Const Build Mater 2024;435:136775. [CrossRef]

[9] Hamada HM, Al-Attar A, Abed F, Beddu S, Humada AM, Majdi A, Thomas B S. Enhancing sustainability in concrete construction: a comprehensive review of plastic waste as an aggregate material. Sustain Mater Technol 2024;40:e00877. [CrossRef]

[10] Xian X, Mahoutian M, Zhang D, Shao Y. Development of wet-cast Portland-cement-free concrete based on steel slag and ambient-pressure carbonation activation. Resour Conserv Recycl 2024;203:107455. [CrossRef]

[11] Wang J, Ren C, Huang T, Li X, Cao W, Zhu Y, Liu Z. Performances of concrete with binder and/or aggregates replacement by all-solid waste materials. J Clean Prod 2024;450:141929. [CrossRef]

[12] Niri AJ, Poelzer GA, Zhang SE, Rosenkranz J, Pettersson M, Ghorbani Y. Sustainability challenges throughout the electric vehicle battery value chain. Renew Sustain Energy Rev 2024;191:114176. [CrossRef]

[13] Maaze MR, Shrivastava S. Design optimization of a recycled concrete waste-based brick through alkali activation using Box-Behnken design methodology. J Build Eng 2023;75:106863. [CrossRef]

[14] Uratani JM, Griffiths S. A forward looking perspective on the cement and concrete industry: implications of growth and development in the Global South. Energy Res Soc Sci 2023;97:102972. [CrossRef]

[15] Hanifa M, Agarwal R, Sharma U, Thapliyal PC, Singh LP. A review on CO2 capture and sequestration in the construction industry: emerging approaches and commercialised technologies. J CO2 Util 2023;67:102292. [CrossRef]

[16] Schneider M, Hoenig V, Ruppert J, Rickert J. The cement plant of tomorrow. Cem Concr Res 2023;173:107290. [CrossRef]

[17] Knight KA, Cunningham PR, Miller SA. Optimizing supplementary cementitious material replacement to minimize the environmental impacts of concrete. Cem Concr Compos 2023;139:105049. [CrossRef]

[18] Singh RP, Vanapalli KR, Cheela VRS, Peddireddy SR, Sharma HB, Mohanty B. Fly ash, GGBS, and silica fume based geopolymer concrete with recycled aggregates: properties and environmental impacts. Const Build Mater 2023;378:131168. [CrossRef]

[19] Kanagaraj B, Lubloy E, Anand N, Hlavicka V, Kiran T. Investigation of physical, chemical, mechanical, and microstructural properties of cement-less concrete–state-of-the-art review. Const Build Mater 2023;365:130020. [CrossRef]

[20] Magesh B, Kumar VS, Raghunath PN, Suguna K. Structural performance of Nano alumina-based RC element with polypropylene fibre and GGBS: an experimental assessment. Sustain Energy Technol Assessments 2023;57:103290. [CrossRef]

[21] Amran M, Onaizi AM, Makul N, Abdelgader HS, Tang WC, Alsulami BT, Gamil Y. Shrinkage mitigation in alkali-activated composites: a comprehensive insight into the potential applications for sustainable construction. Results Eng 2023;20:101452. [CrossRef]

[22] García Del Ángel GDJ, Cabrera R, Rolón J, Pichardo R, Thomas García C. Systematic review on the use of waste foundry sand as a partial replacement of natural sand in concrete. Const Build Mater 2024;430:136460. [CrossRef]

[23] Qin J, Yi Y. Use of gasification fly ash, sodium carbonate, and ground granulated blast-furnace slag for soft clay stabilization. Const Build Mater 2024;426:136072. [CrossRef]

[24] Wang Z, Shui Z, Sun T, Hu T, Xiao X, Fan J. Reutilization of gangue wastes in phosphogypsum-based excess-sulphate cementitious materials: effects of wet co-milling on the rheology, hydration and strength development. Const Build Mater 2023;363:129778. [CrossRef]

[25] Reddy RRK, Yaragal SC, Sagar Srinivasa A. One-part eco-friendly alkali-activated concrete–An innovative sustainable alternative. Const Build Mater 2023;408:133741. [CrossRef]

[26] Xia P, Khan S, Hassam M, Sohaib M, Gong F, Zhao Y. Optimal utilization of low-quality construction waste and industrial byproducts in sustainable recycled concrete. Const Build Mater 2024;428:136362. [CrossRef]

[27] Ahmad J, Arbili MM, Alabduljabbar H, Deifalla AF. Concrete made with partially substitution corn cob ash: A review. Case Stud Constr Mater 2023;18:e02100. [CrossRef]

[28] Hamsashree Pandit P, Prashanth S, Katpady DN. Durability of alkali-activated fly ash-slag concrete-state of art. Innov Infrastruct Solut 2024;9:222. [CrossRef]

[29] Zhao C, Li Z, Peng S, Liu J, Wu Q, Xu X. State-of-the-art review of geopolymer concrete carbonation: from impact analysis to model establishment. Case Stud Constr Mater 2024:e03124. [CrossRef]

[30] Sun T, Li Z, Wang Z, Liu Y, Tang P, Deng Y. Optimization on hydration efficiency of an all-solid waste binder: carbide slag activated excess-sulphate phosphogypsum slag cement. J Build Eng 2024;86:108851. [CrossRef]

[31] Padavala SSA B, Kode VR, Dey S. Sustainable concrete development towards the eco-friendly construction: enhancing the strength and durability by using fly ash and silica fume. J Build Pathol Rehabil 2024;9:50. [CrossRef]

[32] Thorne J, Bompa DV, Funari MF, Garcia-Troncoso N. Environmental impact evaluation of low-carbon concrete incorporating fly ash and limestone. Clean Mater 2024;12:100242. [CrossRef]

[33] Pushpalal D, Danzandorj S, Bayarjavkhlan N, Nishiwaki T, Yamamoto K. Compressive strength development and durability properties of high-calcium fly ash incorporated concrete in extremely cold weather. Const Build Mater 2022;316:125801. [CrossRef]

[34] Silva YF, Delvasto S. Durability of self-compacting concrete with addition of residue of masonry when exposed to carbonation and chlorides mediums. Const Build Mater 2021;297:123817. [CrossRef]

[35] Shi X, Yao Y, Wang L, Zhang C, Ahmad I. A modified numerical model for predicting carbonation depth of concrete with stress damage. Const Build Mater 2021;304:124389. [CrossRef]

[36] Vediyappan S, Chinnaraj PK, Hanumantraya BB, Subramanian SK. An experimental investigation on geopolymer concrete utilising micronized biomass silica and GGBS. KSCE J Civ Eng 2021;25:2134–2142. [CrossRef]

[37] Zhao C, Li J, Zhu Z, Guo Q, Wu X, Wang Z, Zhao R. Research on the carbonation resistance and carbonation depth prediction model of fly ash-and slag-based geopolymer concrete. KSCE J Civ Eng 2024;28:2802–2817. [CrossRef]

[38] Lim YY, Pham TM. Influence of Portland cement on performance of fine rice husk ash geopolymer concrete: strength and permeability properties. Const Build Mater 2021;300:124321. [CrossRef]

[39] Çelik Z, Bingöl AF, Ağsu AS. Fresh, mechanical, sorptivity and rapid chloride permeability properties of self-compacting concrete with silica fume and fly ash. Iran J Sci Technol 2022;46:789–799. [CrossRef]

[40] Kumar R, Verma M, Dev N. Investigation on the effect of seawater condition, sulphate attack, acid attack, freeze–thaw condition, and wetting–drying on the geopolymer concrete. Iran J Sci Technol 2022;46: 2823–2853. [CrossRef]

[41] Somasekharaiah HM, Shobha MS, Mallikarjuna HM. Mechanical properties and acid attack test of hybrid fiber reinforced high performance concrete for fly ash based mineral admixture. Mater Today Proc 2022;51:742–749. [CrossRef]

[42] Sahoo S, Parhi PK, Panda BC. Durability properties of concrete with silica fume and rice husk ash. Clean Eng Technol 2021;2:100067. [CrossRef]

[43] Türköz M, Umu SU, Öztürk O. Effect of silica fume as a waste material for sustainable environment on the stabilization and dynamic behavior of dispersive soil. Sustainability 2021;13:4321. [CrossRef]

[44] El Ouni MH, Shah SHA, Ali A, Muhammad S, Mahmood MS, Ali B, Raza A. Mechanical performance, water and chloride permeability of hybrid steel-polypropylene fiber-reinforced recycled aggregate concrete. Case Stud Constr Mater 2022;16:e00831. [CrossRef]